Int. J. Heat Mass Transfer. Vol. 15, pp. 513–525. Pergamon Press 1972. Printed in Great Britain

AN EXPERIMENTAL INVESTIGATION OF NATURAL CONVECTION IN MERCURY AT LOW GRASHOF NUMBERS

B. H. CHANG† and R. G. AKINS

Department of Chemical Engineering, Kansas State University, Manhattan, Kansas, U.S.A.

(*Received* 1 *March* 1971 *and in revised form* 27 *May* 1971)

Abstract—This paper presents the results of an experimental investigation of natural convection from a uniformly heated, vertical flat plate immersed in mercury. Data were obtained at low Grashof numbers particularly.

Temperature profiles about the plate were measured with a copper–constantan thermocouple and the results presented on dimensionless plots. The experimental results deviated from the similarity solution of the boundary layer equations and these deviations are shown to depend on the distance up the plate, the heat flux, and the Nusselt number. A qualitative comparison is made with the predictions of a perturbation analysis.

Present experimental data (Gr_x^* from 1 to 10^8) were correlated to give a relationship between Nu_x and Gr_x^*, and this compared with analytical predictions as well as other correlations (Gr_x^* from 10^4 to 10^9). Positive deviation of experimental Nu_x from the theoretical value was estimated to be about 20 per cent at $Gr_x^* = 2 \times 10^4$ and $Pr = 0.024$.

NOMENCLATURE

C_p, specific heat at constant pressure [Btu/lb°F];

Gr_x, local Grashof number, $\frac{g\beta(T_w - T_\infty)x^3}{\nu^2}$ [dimensionless];

Gr_x^*, modified local Grashof number, $\frac{g\beta q x^4}{k\nu^2} = Gr_x Nu_x$, [dimensionless];

Gr_L^*, modified Grashof number, $\frac{g\beta q L^4}{k\nu^2}$ [dimensionless];

g, gravitational acceleration [ft/s^2];

h_x, local heat transfer coefficient [Btu/h ft^2°F];

L, height of plate [ft];

Nu_x, local Nusselt number, $\frac{h_x x}{k}$ or $\frac{qx}{k(T_w - T_\infty)}$, [dimensionless];

Pr, Prandtl number, $C_p\mu/k$ [dimensionless];

q, heat flux at the wall [Btu/h ft^2];

T, temperature [°F];

T_w, wall temperature [°F];

T_∞, bulk temperature [°F];

x, vertical distance up the plate from the leading edge [ft];

y, horizontal distance away from the plate [ft].

Greek symbols

β, thermal expansion coefficient [1/°F];

η, similarity variable, dimensionless distance, $\frac{y}{x}\left(\frac{Gr_x^*}{5}\right)^{\frac{1}{5}}$;

σ, standard deviation;

μ, viscosity [lb$_m$/ft s];

ν, kinematic viscosity [ft^2/s].

† Present address: Department of Chemical Engineering, University of Louisville.

E

INTRODUCTION

THE BOUNDARY layer assumptions used to simplify the coupled equations of motion, energy, and continuity which describe laminar natural convection heat transfer from a vertical flat plate, have been experimentally verified [11] for liquid metals in a moderate range of local modified Grashof number (10^6–10^9). There has not been an experimental investigation on natural convection in liquid metals at low Grashof number ($<10^6$) where appreciable deviations from the boundary layer theory have been predicted by perturbation analyses [4, 7]. Therefore, the purpose of this study was to obtain the experimental temperature profiles and to compare the results with those predicted by theoretical analyses.

In 1904, Prandtl [1] simplified the Navier–Stokes equations by dividing the flow into two regions: a thin boundary layer along the solid surface where viscous effects were important and the velocity gradient normal to the wall was large, and a bulk flow region where viscous effects could be neglected.

Sparrow and Gregg [2] analyzed laminar free convection for a vertical flat plate by determining a similarity transformation which reduced the boundary layer equations to a pair of ordinary differential equations, which were solved numerically for Prandtl numbers of 0·1, 1, 10 and 100. Chang *et al.* [3] extended Sparrow and Gregg's solutions to Prandtl numbers of 0·1 and 0·03 for liquid metals.

In 1964, Yang and Jerger [4] applied a perturbation analysis to natural convection from an isothermal plate. They expected the perturbation solution to be more accurate than the similarity solution at moderate Grashof numbers. Suriano, Yang and Donlon [5] used the perturbation analysis for the free convection at the extremely small Grashof numbers (less than one), and Suriano and Yang [6] extended the previous work to small Grashof numbers (Rayleigh number from 1 up to 300) with Prandtl numbers of 0·72 and 10.

Chang, Akins and Bankoff [7] applied a perturbation analysis to the case of constant heat flux plate. They found, for low Prandtl numbers, that the dimensionless temperature profiles were no longer a single line (as with the boundary layer solution), but varied with position on the plate and the Grashof number. They presented first-order perturbation solutions for Prandtl numbers of 0·01 and 0·03.

Sparrow and Guinle [8], using the perturbation technique, investigated the deviations for classical free convection boundary layer theory at low Prandtl numbers. They evaluated effects of transverse pressure gradient and streamwise second derivatives on the local heat transfer from an isothermal vertical flat plate. Grashof numbers delineating the threshold of significant departures from the classical boundary-layer results were given for Prandtl numbers of 0·03 and 0·003, which bound the liquid metal range, and also for $Pr = 0{\cdot}733$ (air) to demonstrate that the factors under consideration were negligible outside metal range.

In 1939, Saunders [9] obtained experimental data for heat transfer from a constant temperature vertical plate in mercury and in water. Since the plate he used was a heated portion of a wall, and it had no leading and trailing edges, it was difficult to analyze the data. The data also lacked accuracy.

Julian and Akins [10] carried out experiments on natural convection from a uniformly heated, vertical flat plate in mercury and in water in the range of moderate Grashof numbers (Gr_x^* from 10^4 to 10^9). The experimental results were in good agreement with the similarity solutions of boundary layer equations except that the data appeared to be slightly low. They attempted to check the perturbation prediction that the temperature profiles would depend on the vertical distance on the plate as well as on the Grashof number, but a detailed investigation failed because of experimental errors. In the present work, data have been taken in the range of Grashof number from 1 to 10^8 and the perturbation predictions have been checked qualitatively.

EXPERIMENTAL APPARATUS AND INSTRUMENTATION

The experimental equipment was essentially the same as that used by Julian [11]. The only modification was the addition of an $X-Y$ plotter for added amplification. The apparatus consisted of a container for mercury, a heated vertical plate, a thermocouple, and a mechanism for accurately positioning the thermocouple with respect to the plate.

The container was 7 in. wide, 9 in. long, and 13 in. high, and was made of type 410 stainless steel. The top, which was open, was covered with stainless plate which carried the plate supports and the thermocouple positioning mechanism. The plate was made of type 302 stainless steel, and was 2 in. high, 4 in. wide and 0·004 in. thick. It was coated with a plasticized acrylic resin to insulate it electrically from the mercury. The plate was located in the center of the container and was heated electrically with direct current. The plate dissipated heat from both sides, i.e. 16 in^2 of surface, whereas the mercury dissipated this heat through approximately 500 in^2. The heat was rejected to constant temperature room air and, for the very low heat transfer rates used in this work, this was found to be more satisfactory than the use of a constant temperature water bath surrounding the mercury container.

The thermocouple was copper–constantan and was encased in a 0·014 in. diameter, type 302 stainless steel sheath. The thermocouple pointed into the flow, i.e. downward and was bent slightly so that the tip would make contact with the plate surface. The thermocouple could be positioned vertically on the plate to within $\pm 0{\cdot}001$ in. The horizontal movement (toward or away from the plate) was accomplished using a synchronous motor—the speed of the thermocouple being $\frac{1}{16}$ of an in. per min and its position from the plate was known to be $\pm 0{\cdot}001$ in. at all times.

The small voltage generated between the thermocouple in mercury and a similar one in ice water (reference junction) was amplified by a Sanborn, Model 350-1500, low-level preamplifier and 350 amplifier, then further amplified and plotted by an EAI, Model 1130, $X-Y$ plotter. The other input to the plotter came from a potentiometer attached to the shaft of the synchronous motor used to move the thermocouple.

EXPERIMENTAL PROCEDURE AND DATA ANALYSIS

The thermocouple was located vertically at the point of interest on the plate by turning the vertical screw arrangement. All the profiles were plotted starting from the plate and moving to the bulk, and then reversing the motor, from the bulk to the plate. In this manner, two almost identical profiles were superposed so that steady state as well as the effects of the direction of movement could be checked. The two profiles generally were not identical, however, the difference was always less than 4 per cent of overall temperature difference. The plate surface temperature was also found to vary within same order of magnitude. The plotted distance between the plate and a given position in the bulk was always shorter when moving from the plate than it was when moving toward the plate. This was thought to be due to the thermocouple probe sticking slightly to the plate or requiring a slight pressure in order to contact the plate firmly. The difference in the apparent plate location was never more than 0·5 per cent of the total profile distance. The profiles toward and away from the plate were averaged and the data were taken from this averaged profile.

The reference temperature for evaluation of physical properties was calculated from the wall and bulk temperatures as Sparrow [12] recommended, i.e. a weighted average of 70 per cent of wall temperature and 30 per cent of the bulk temperature.

Dimensionless data points (usually 20 per profile) were fitted to first- to sixth-order polynomial curves in order to examine the predicted trends of dimensionless profiles, and then the polynomial curve whose standard deviation was the smallest was chosen as a final dimensionless plot. Careful attention was paid to the fitting procedure to insure that the conclusions drawn were not a result of a particular polynomial fit used.

EXPERIMENTAL RESULTS

(a) *Overall dimensionless temperature distribution*

The results of experimental runs at various heat fluxes and vertical positions on the plate are presented in a dimensionless plot (Fig. 1).

Figure 1 is to show the general location of the data. As can be seen, much of the data fall below the boundary-layer solution results. No particular experimental runs are identified in this figure, but the data showed that the points far below the dashed line came from runs taken at very low Grashof numbers and/or close to the leading edge. A more detailed examination of these shifts away from the boundary-layer solution is made in the next sections.

(b) *Dependence of dimensionless profiles on the vertical distance on the plate*

Figures 2–5 show the dependence of dimen-

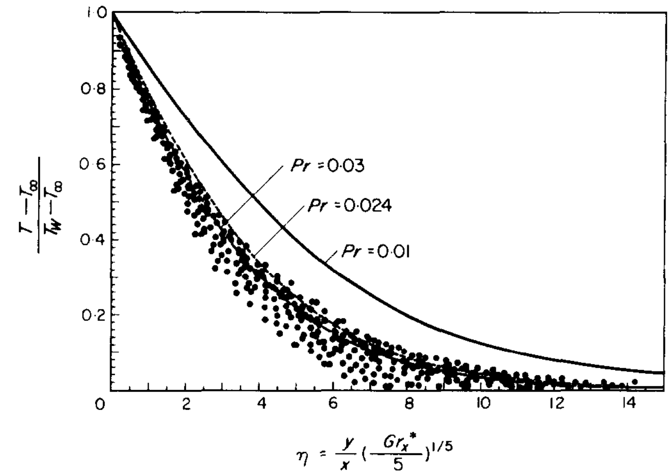

FIG. 1. Overall dimensionless temperature distribution.
Heat flux: from 26 to 1150 Btu/ft^{2}h
Gr_x^*: from 1 to 10^8
Pr: 0·024
Vertical position: $x/L = \frac{1}{64}, \frac{1}{32}, \frac{1}{16}, \frac{1}{8}, \frac{1}{2}, \frac{3}{4}$ and $\frac{7}{8}$.

The two solid lines in this figure are the boundary-layer solutions for Prandtl numbers of 0·01 and 0·03, which were obtained by Chang *et al.* [3]. The dashed line is also a boundary-layer solution for $Pr = 0{\cdot}024$, which was the condition of this work. The similarity equations for this Prandtl number were solved numerically on an IBM 360/50 computer.

sionless temperature profiles on the distance up the plate at constant heat fluxes. Figures 2 and 3 include profiles for the lower and upper parts of the plate, respectively, at the same heat flux. Likewise, Figs. 4 and 5 correspond in plate position to the Figs. 2 and 3, respectively, but are for a higher heat flux. At one level of heat flux (constant Gr^*_x) several profiles were

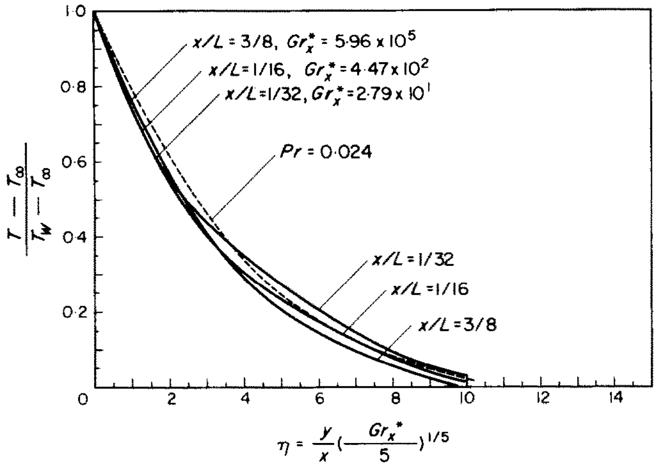

FIG. 2. Dimensionless temperature profiles for a heat flux of 87 Btu/ft^{2}h ($Gr_L^* = 2.93 \times 10^7$).

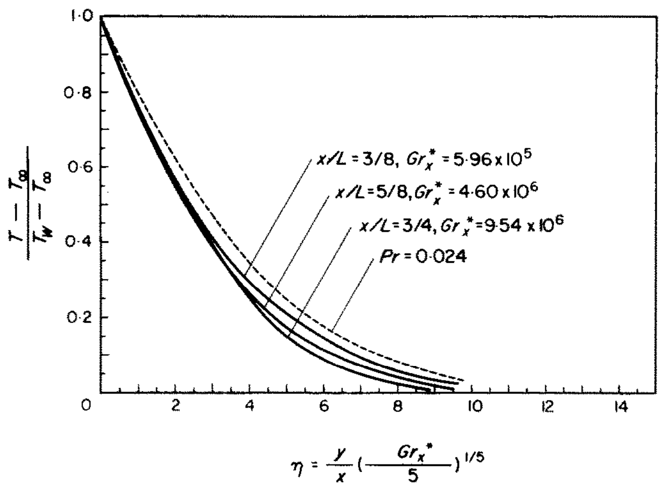

FIG. 3. Dimensionless temperature profiles for a heat flux of 87 Btu/ft^{2}h ($Gr_L^* = 2.93 \times 10^7$).

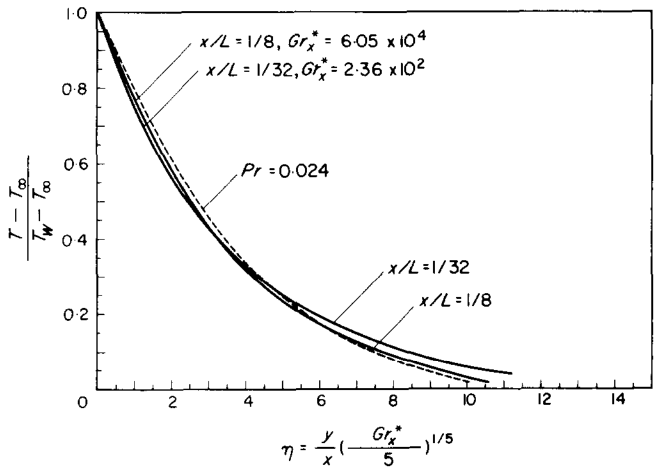

FIG. 4. Dimensionless temperature profiles for a heat flux of 735 Btu/ft^{2}h (Gr^*_L = 2·52 × 10^8).

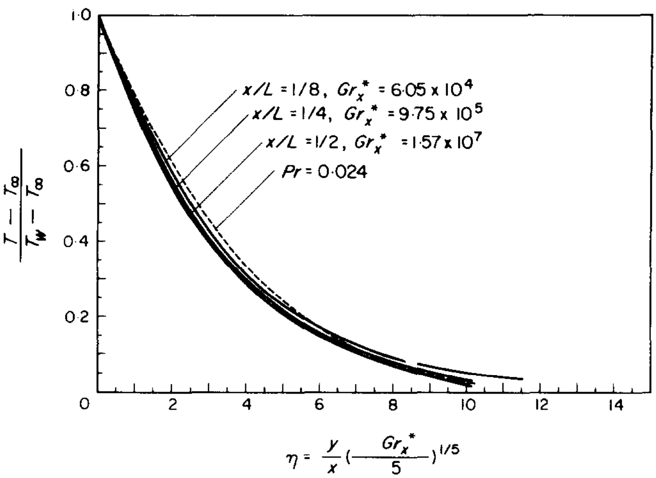

FIG. 5. Dimensionless temperature profiles for a heat flux of 735 Btu/ft^{2}h (Gr^*_L = 2·52 × 10^8).

obtained at various positions (x) up the plate. The dashed lines in the figures are the boundary layer solution for $Pr = 0{\cdot}024$ and the solid lines represent the best polynomial fit of each experimental data set. These profiles can be compared with those of the first-order perturbation analysis [7] (Figs. 6 and 7 for temperature and velocity profiles, respectively).

predicted by the perturbation analysis, although it does show (see Fig. 7) that the velocity profiles cross each other in the same general range of η.

At a given heat flux, increases in x up to a certain value (reversal point) shifted the temperature profiles toward the boundary-layer solution, but farther increases in x above this

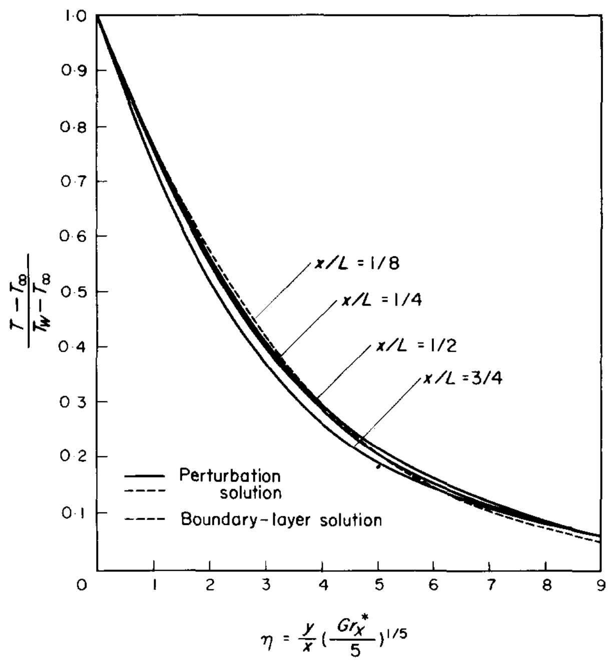

FIG. 6. Comparison of temperature profiles for $Pr = 0{\cdot}03$ when $Gr_x^* = 10^7$.

First, looking at Figs. 2 and 4 for the lower part of the plate as compared with Fig. 6, we can see general agreement at the smaller values of the dimensionless distance η. The profiles at increasing x approach the boundary layer solution. For larger values of dimensionless distance, however, the trend with x is reversed and whether or not the profiles approach the boundary layer solution is not very clear. The crossing of the temperature profiles was not

value caused the profiles to move further from the boundary layer solution. Figures 3 and 5 show the temperature profiles above this reversal point did not follows the general trend of the perturbation prediction. Close examination of the dimensionless plots indicates that the reversal point depends on the heat flux: it goes down as the heat flux goes up. It was experimentally found that the reversal points were $\frac{3}{8}$, $\frac{1}{4}$, $\frac{1}{4}$ and $\frac{1}{8}$ of the plate height for the heat fluxes

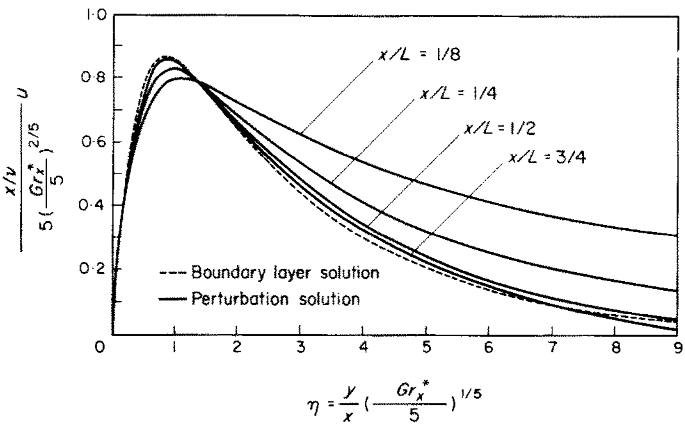

FIG. 7. Comparison of velocity profiles for $Pr = 0{\cdot}03$ when $Gr_L^* = 10^7$.

of 87, 121, 354 and 735 Btu/ft^{2}h, respectively. It should be noted that since the data were obtained at several fixed positions in x, exact reversal point for each heat flux was not determined. However, the general trend is obvious.

(c) *Dependence of the dimensionless profiles on heat flux*

Figures 8–10 show the effects of heat flux on the profiles at various fixed vertical positions. Since x was fixed, the heat flux was directly proportional to Gr_x^* and Gr_L^*. Generally, the profiles approach the boundary layer solution with increases in heat flux. This is consistent with the theory that the boundary layer assumptions are increasingly applicable as the Grashof number increases.

(d) *Dependence of dimensionless profiles on Nusselt number for constant* Gr_x^*

A constant modified Grashof number could

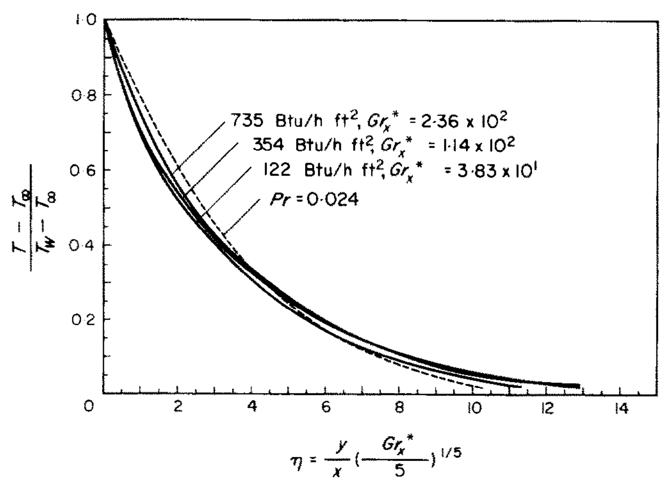

FIG. 8. Dimensionless temperature profiles at $x/L = \frac{1}{16}$.

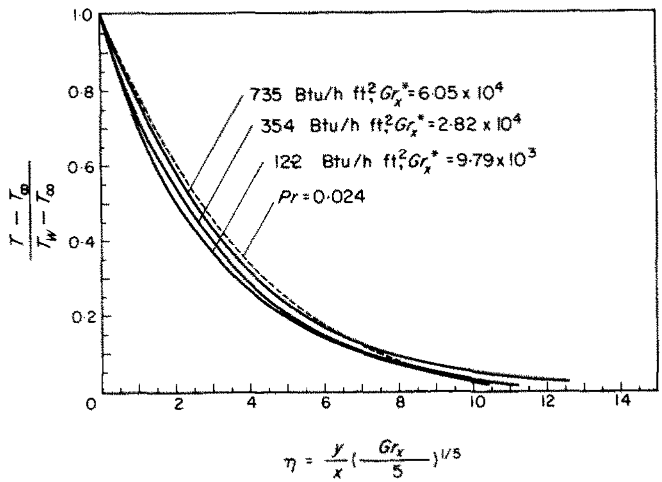

FIG. 9. Dimensionless temperature profiles at $x/L = \frac{1}{8}$.

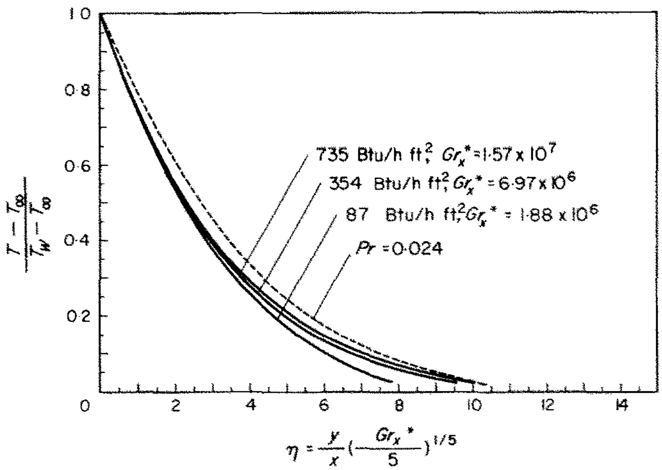

FIG. 10. Dimensionless temperature profiles at $x/L = \frac{1}{2}$.

be obtained experimentally by changing x and q properly. There were experimental difficulties in obtaining exactly the same values of Gr_x^* with different x's and q's, so that constancy of Gr_x^* here implies deviations of less than 5 per cent. Dimensionless profiles are presented in Figs. 11–13 with Nu_x as a parameter and Gr_x^* constant. Since Gr_x^* is a function of q and x it is not possible to use either of them alone as a parameter, therefore the local Nusselt number Nu_x serves as a convenient parameter, since it is a function of both. Figures 11–13 show that at constant Gr_x^*, the profiles deviate more from the boundary-layer theory as the local Nusselt number increases. This result is in agreement with Sparrow and Guinle's analysis [8], i.e.

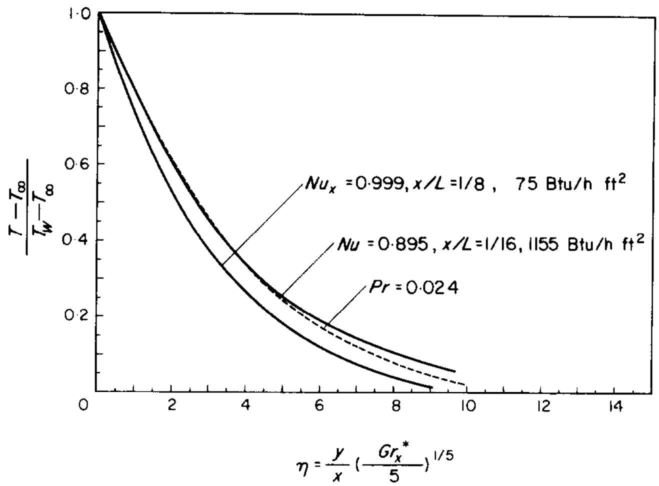

FIG. 11. Dimensionless temperature profiles at $Gr_x^* = 6 \times 10^3$.

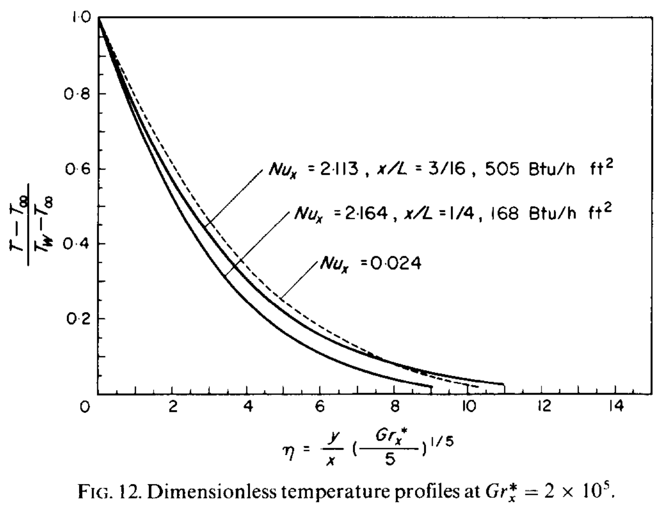

FIG. 12. Dimensionless temperature profiles at $Gr_x^* = 2 \times 10^5$.

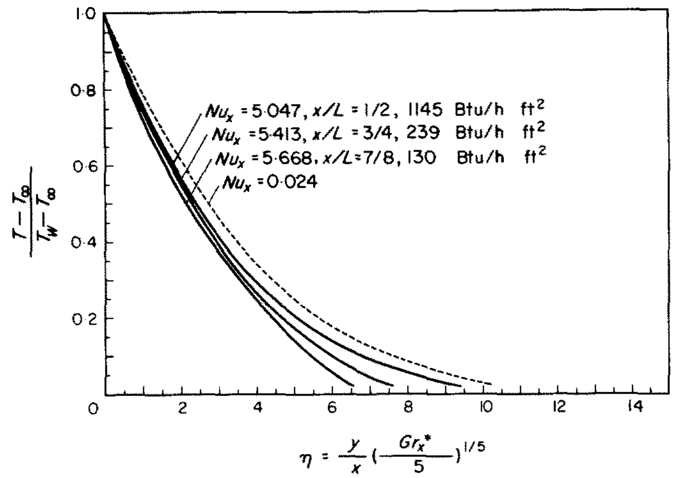

FIG. 13. Dimensionless temperature profiles at $Gr_x^* = 2.5 \times 10^7$.

the actual heat transfer is greater than the heat transfer predicted by the boundary-layer theory especially for small values of Gr_x^*. Detailed heat transfer data is presented in the following section, and the deviation from theory can be seen more clearly.

(e) *Heat transfer results*

Figure 14 presents the local Nusselt numbers plotted against the modified Grashof number. The dashed line represents Sparrow and Gregg's theoretical correlation from the boundary layer solution, i.e.

$$\frac{Gr_x^{*0.2}}{Nu_x} = 6.3 \qquad \text{(for } Pr = 0.024\text{)}.$$

Julian's [11] experimental heat transfer correlation is included in Fig. 14. It is of the form

$$\frac{Gr_x^{*0.188}}{Nu_x} = 5.1 \quad (Pr = 0.022 \text{ and } Gr_x^* = 10^4 \rightarrow 10^9)$$

with the standard deviation (σ) of 0.021. Also included is Saunders' data [9] which are the only available heat transfer data in addition to Julian's.

For the present work, data from sixty runs were correlated to give

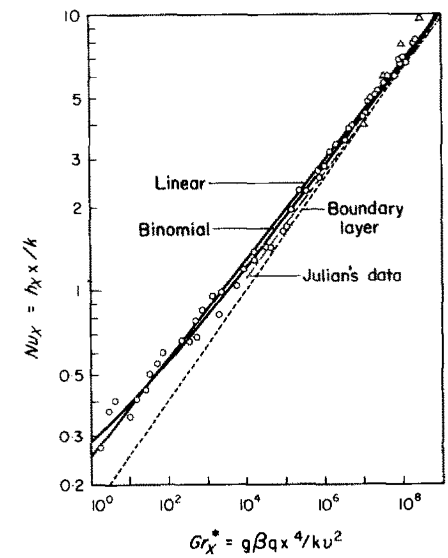

FIG. 14. Correlations between the Nusselt and Grashof numbers for natural convection from a flat, vertical plate at constant heat flux

---- Boundary-layer solution, Sparrow and Gregg [2]

–.–. Julian's experimental correlation [10] $(Gr_x^{*0.188}/Nu_x) = 5.1, \sigma = 0.021$

——— *Present experimental correlations*

Linear: $(Gr_x^{*0.178}/Nu_x) = 4.03, \sigma = 0.033$

Binomial: $\log Nu_x = -0.551 + 0.145 \log Gr_x^* + 0.004 + 0.004 (\log Gr_x^*)^2, \sigma = 0.028.$

○ Data from present work

△ Data from Saunders [9].

(1) Linear correlation for Gr_x^* from 1 to 10^8:

$$\frac{Gr_x^{*0.178}}{Nu_x} = 4.03, \qquad \sigma = 0.033$$

(2) Linear correlation for Gr_x^* from 10^4 to 10^8:

$$\frac{Gr_x^{*0.188}}{Nu_x} = 4.69, \qquad \sigma = 0.022$$

(3) Linear correlation for Gr_x^* from 1 to 10^4:

$$\frac{Gr_x^{*0.157}}{Nu_x} = 3.60, \qquad \sigma = 0.041$$

(4) Binomial correlation for Gr_x^* from 1 to 10^8:

$$\log Nu_x = -0.551 + 0.145 \log Gr_x^* + 0.004 (\log Gr_x^*)^2, \qquad \sigma = 0.028$$

The curve for the binomial overall correlation was almost the same as the combination of two straight lines for the high and low range linear correlations.

Examination of the binomial correlation shows that experimental values of Nu_x at constant Gr_x^* were generally greater than their theoretical values, and that as Gr_x^* decreased, the positive deviation increased. As expected, at high Grashof numbers the heat transfer approached that predicted by the boundary layer theory. Sparrow and Guinle estimated the deviation from the theoretical heat transfer to be 5 per cent (greater) at $Gr_x = 2 \times 10^4$ and $Pr = 0.03$ for the case of the isothermal plate. From the present results we find a 20 per cent positive deviation at $Gr_x^* = 2 \times 10^4$ and $Pr = 0.024$. Direct quantitative comparison can not be made, of course, because of the different conditions.

CONCLUSIONS

Departures from classical free convection boundary-layer theory have been experimentally shown in the range of Grashof number from 1 to 10^8 in mercury ($Pr = 0.024$). Perturbation predictions that temperature profiles should depend upon the vertical distance up the plate as well as the Grashof number, also have been verified. However, the magnitude and direction of the deviations found experimentally were not always in agreement with the perturbation results. In particular, the experimental temperature profiles crossed each other when plotted as a parameter of vertical position, whereas the perturbation analysis predicts no such crossing. The discrepancy was caused either by some experimental error or (more likely) from the fact that higher order perturbation terms are required for an accurate prediction. Of course, it is possible for the perturbation analysis to give poor results no matter how many terms are used, but the fact that it did give reasonable results in some areas shows its value.

The heat transfer results show positive deviations at all Grashof numbers with the deviation increasing as the Grashof number decreased. As expected, the heat transfer approached the boundary layer prediction at high Grashof numbers. The heat transfer correlation determined through the boundary-layer assumptions seems to be completely satisfactory for any practical work with liquid metals, since it gives a slightly conservative result.

REFERENCES

1. L. Prandtl, Uber Flussigkeitsbewegun bei sehr kleiner Reibung *Proceedings of Third International Mathematical Congress*, Heideberg, 1904; reprinted in *Vier-Abhdl. zur Hydro-Aerodynamik*, Gottingen, 1927; NACA TN-452 (1955).
2. E. M. Sparrow and J. L. Gregg, Laminar free convection from a vertical plate with uniform heat flux, *Trans. Am. Soc. Mech. Engrs* **78**, 435–440 (1956).
3. K. S. Chang, R. G. Akins, L. Burris and S. G. Bankoff, Free convection of a low Prandtl number fluid in contact with a uniformly heated vertical plate, Argonne National Laboratory ANL-1835 (1964).
4. K. T. Yang and E. W. Jerger, First-order perturbations of laminar free convection boundary layers on a vertical plate, *J. Heat Transfer* **86C**, 107–115 (1964).
5. F. J. Suriano, K. T. Yang and J. A. Donlon, Laminar free convection along a vertical plate at extremely small Grashof numbers, *Int. J. Heat Mass Transfer* **8**, 815–831 (1965).
6. F. J. Suriano and K. T. Yang, Laminar free convection about vertical and horizontal plates at small and moderate Grashof numbers, *Int. J. Heat Mass Transfer* **11**, 473–490 (1968).
7. K. S. Chang, R. G. Akins and S. G. Bankoff, Free

convection of a liquid metal from a uniformly heated vertical plate, *I/EC Fundamentals* **5**, 26–37 (1966).
8. E. M. SPARROW and LUIZ DE MELLO F. GUINLE, Deviations from classical free convection boundary-layer theory at low Prandtl numbers, *Int. J. Heat Mass Transfer* **11**, 1403–1406 (1968).
9. O. A. SAUNDERS, Natural convection in liquids, *Proc. R. Soc., Lond.* **A172**, 55–71 (1939).
10. D. V. JULIAN and R. G. AKINS, Experimental investigation of natural convection heat transfer to mercury, *I/EC Fundamentals* **8**, 641–646 (1969).
11. D. V. JULIAN, An experimental study of natural convection heat transfer from a uniformly heated vertical plate immersed in mercury, Ph.D. Thesis, Kansas State University (1967).
12. E. M. SPARROW, Free convection with variable properties and variable wall temperatures, Ph.D. Thesis, Harvard University (1956).

RECHERCHE EXPÉRIMENTALE SUR LA CONVECTION NATURELLE DANS DU MERCURE À DES FAIBLES NOMBRES DE GRASHOF

Résumé—Cet article présente les résultats d'une recherche expérimentale sur la convection naturelle à partir d'une plaque plane verticale uniformément chauffée et immergée dans du mercure. On a obtenu des résultats pour des nombres de Grashof particulièrement bas.

On a mesuré des profils de température au voisinage de la plaque avec un thermocouple cuivre-constantan et les résultats sont présentés graphiquement sous forme adimensionnelle. On montre que les résultats expérimentaux s'ècartent de la solution de similarité des équations de la couche limite et que ces déviations dépendent de la hauteur à partir de la plaque, du flux thermique et du nombre de Nusselt. Une comparaison qualitative a été faite avec les prédictions d'une analyse de perturbation.

Des résultats expérimentaux présents (Gr_x^* de 1 à 10^8) ont été mis en corrélation afin de donner une loi entre Nu_x et Gr_x, et celle-ci a été comparée aux prédictions analytiques aussi bien qu'à d'autres relations (Gr_x^* de 10^4 à 10^9). L'écart positif du Nu_x expérimental à partir de la valeur théorique a été estimé pour être d'à peu près 20% pour $Gr_x^* = 2 \times 10^4$ et $Pr = 0{,}024$.

EXPERIMENTELLE UNTERSUCHUNG DER NATÜRLICHEN KONVEKTION IN QUECKSILBER BEI KLEINEN GRASHOF-ZAHLEN

Zusammenfassung—Es wird über die Ergebnisse einer experimentellen Untersuchung der freien Konvektion in Quecksilber an einer gleichmässig beheizten, vertikalen, ebenen Platte berichtet.

Die Temperaturprofile entlang der Platte wurden mit einem Thermoelement aus Kupfer-Konstantan gemessen und die Ergebnisse sind in dimensionsloser Form dargestellt. Die Versuchsergebnisse weichen von der Ähnlichkeitslösung der Grenzschichtgleichungen ab.

Es wird gezeigt, dass diese Abweichungen abhängig sind vom Abstand zur Platte, dem Wärmestrom und der Nusselt-Zahl. Es wird ein qualitativer Vergleich angestellt mit Rechnungen nach einer Störungsanalyse.

Die vorliegenden Versuchswerte ($1 \leqslant Gr_x^* < 10^8$) wurden abhängig von Nu_x gemacht und diese Abhängigkeit verglichen sowohl mit analytischen Vorhersagen als auch mit anderen Gleichungen ($10^4 \leqslant Gr_x^* \leqslant 10^9$).

Die positive Abweichung der experimentellen Nu_x gegenüber dem theoretischen Wert wurde auf 20% geschätzt bei $Gr_x^* = 2 \cdot 10^4$ und $Pr = 0{,}024$.

ЭКСПЕРИМЕНТАЛЬНОЕ ИССЛЕДОВАНИЕ ЕСТЕСТВЕННОЙ КОНВЕКЦИИ В РТУТИ ПРИ НИЗКИХ ЧИСЛАХ ГРАСГОФА

Аннотация—В данной статье представлены результаты экспериментального изучения естественной конвекции от равномерно нагретой, вертикальной плоской пластины, погружённой в ртуть. Данные были получены, в частности, при низких числах Грасгофа.

Температурные профили у пластины измерялись медь-константановой термопарой, и результаты представлены в безразмерном виде. Экспериментальные результаты отклонялись от автомодельного решения уравнений пограничного слоя, и показано, что эти отклонения зависят от расстояния вверх по пластине, теплового потока и числа Нуссельта. Приводится качественное сравнение с данными по исследованию возмущённого движения.

Проведена корреляция представленных экспериментальных данных (Gr_x^* от 1 до 10^8) и получено соотношение между Nu_x и Gr_x^*, которое сравнивалось с аналитическими расчётами и другими корреляциями (Gr_x^* от 10^4 до 10^9). Положительное отклонение экспериментального значения Nu_x от теоретического составляет 20% при $Gr_x^* = 2 \times 10^4$ и $Pr = 0{,}024$.